Title

Adaptive right ventricular performance in response to acutely increased afterload in a lamb model of congenital heart disease: evidence for enhanced Anrep effect

Journal

AJP Heart and Circulatory Physiology, 306(8)

ISSN

0363-6135

Authors

Johnson, Rebecca C
Datar, Sanjeev A
Oishi, Peter E
et al.

Publication Date

2014-04-15

DOI

10.1152/ajpheart.01018.2013

Peer reviewed

Am J Physiol Heart Circ Physiol 306: H1222–H1230, 2014.
First published February 21, 2014; doi:10.1152/ajpheart.01018.2013.

Adaptive right ventricular performance in response to acutely increased afterload in a lamb model of congenital heart disease: evidence for enhanced Anrep effect

Rebecca C. Johnson,[1,2] Sanjeev A. Datar,[1] Peter E. Oishi,[1,2] Stephen Bennett,[1] Jun Maki,[1] Christine Sun,[1] Michael Johengen,[1] Youping He,[1] Gary W. Raff,[3] Andrew N. Redington,[4] and Jeffrey R. Fineman[1,2]

[1]*Department of Pediatrics, University of California, San Francisco, California;* [2]*Cardiovascular Research Institute, University of California, San Francisco, California;* [3]*Department of Surgery, University of California, Davis, California; and* [4]*Division of Cardiology, Hospital for Sick Children, University of Toronto, Toronto, Canada*

Submitted 26 December 2013; accepted in final form 7 February 2014

Johnson RC, Datar SA, Oishi PE, Bennett S, Maki J, Sun C, Johengen M, He Y, Raff GW, Redington AN, Fineman JR. Adaptive right ventricular performance in response to acutely increased afterload in a lamb model of congenital heart disease: evidence for enhanced Anrep effect. *Am J Physiol Heart Circ Physiol* 306: H1222–H1230, 2014. First published February 21, 2014; doi:10.1152/ajpheart.01018.2013.—Patients with pulmonary hypertension associated with congenital heart disease survive longer with preserved right ventricular (RV) function compared with those with primary pulmonary hypertension. The purpose of this study was to test the hypothesis that superior RV performance can be demonstrated, at baseline and when challenged with increased RV afterload, in lambs with chronic left-to-right cardiac shunts compared with control lambs. A shunt was placed between the pulmonary artery and the aorta in fetal lambs (shunt). RV pressure-volume loops were obtained 4 wk after delivery in shunt and control lambs, before and after increased afterload was applied using pulmonary artery banding (PAB). Baseline stroke volume (8.7 ± 1.8 vs. 15.8 ± 2.7 ml, $P = 0.04$) and cardiac index (73.0 ± 4.0 vs. 159.2 ± 25.1 ml·min^{-1}·kg^{-1}, $P = 0.02$) were greater in shunts. After PAB, there was no difference in the change in cardiac index (relative to baseline) between groups; however, heart rate (HR) was greater in controls (168 ± 7.3 vs. 138 ± 6.6 beats/min, $P = 0.01$), and end-systolic elastance (Ees) was greater in shunts (2.63 vs. 1.31 × baseline, $P = 0.02$). Control lambs showed decreased mechanical efficiency (71% baseline) compared with shunts. With acute afterload challenge, both controls and shunts maintained cardiac output; however, this was via maladaptive responses in controls, while shunts maintained mechanical efficiency and increased contractility via a proposed enhanced Anrep effect—the second, slow inotropic response in the biphasic ventricular response to increased afterload, a novel finding in the RV. The mechanisms related to these physiological differences may have important therapeutic implications.

right ventricle; cardiac performance; pressure-volume loops; congenital heart disease; pulmonary hypertension

PULMONARY ARTERIAL HYPERTENSION (PAH) is a rare but devastating disease that carries a significant burden of morbidity and mortality (24). Most investigations have focused on the mechanisms that underlie abnormal pulmonary vascular reactivity and remodeling, which have led to the development of effective therapies with improved survival (13, 16). Likewise, much of the clinical evaluation of patients with PAH is based upon assessments of pulmonary arterial pressure and pulmonary vascular resistance. However, there is growing recognition that indexes of right ventricular (RV) function in patients with PAH, including right atrial pressure and cardiac index, are correlated most closely with survival and functional class (25). In fact, the prognostic significance of RV function across a diverse group of cardiovascular diseases, including pulmonary hypertension (26), left heart failure (6), and congenital heart disease (19) has only recently been recognized. Nonetheless, RV physiology remains relatively understudied, and the pathophysiology of RV functional decline is poorly understood.

Interestingly, in contrast to most patients with primary PAH, patients with PAH associated with congenital heart disease (CHD) have better functional capacity despite equivalent pulmonary artery pressures and advanced pulmonary arteriopathy (8). These patients also have lower right atrial pressures and higher cardiac output. Superior right heart function in these patients may reflect persistence of the fetal RV phenotype, since the presence of an unrestrictive left-to-right shunt anywhere at the post-tricuspid level will apply systemic-level afterload to the RV. In this situation, the RV does not undergo the deconditioning that normally occurs when pulmonary vascular resistance decreases after birth. Consequently, the chronic responses of the RV to increased afterload in PAH associated with CHD appear to be advantageous when compared with earlier RV failure that occurs in other PAH classes, but the physiological and biochemical basis for this observation is, as yet, unknown. A better understanding of the potentially adaptive physiological mechanisms responsible for the preservation of RV function in the setting of PAH associated with CHD may have important therapeutic implications.

Therefore, the purpose of the present study was to test the hypothesis that superior RV performance can be demonstrated, at baseline and when challenged with increased RV afterload, in lambs with chronic left-to-right cardiac shunts compared with age-matched controls. For this study, we used a well-established, clinically relevant lamb model of a congenital cardiac defect with a large left-to-right shunt, created by the in utero placement of an 8-mm aorta-to-pulmonary shunt (shunt lambs). Using RV admittance pressure-volume catheters, we first characterized the differences in cardiac performance between 4-wk-old shunt and control lambs, and then compared their response to an acute increase in RV afterload, over a 4-h period following surgical placement of a pulmonary artery band (PAB).

Address for reprint requests and other correspondence: J. R. Fineman, Dept. of Pediatrics, Univ. of California, San Francisco, CA (e-mail: jeff.fineman@ucsf.edu).

METHODS

Surgical preparation. A total of six pregnant mixed-breed Western ewes (137–141 days gestation, term = 145 days) were anesthetized. Fetal exposure was obtained through the horn of the uterus; a left lateral thoracotomy was performed on the fetal lamb. With the use of side biting vascular clamps, an 8.0-mm vascular graft was anastomosed between the ascending aorta and main pulmonary artery of the fetal lambs. This procedure was previously described in detail (17). Control lambs were either provided by twin gestation ($n = 3$) or age-matched ($n = 3$). Control lambs did not undergo a lateral thoracotomy.

Four weeks after spontaneous delivery shunt and control (3 provided by twin pregnancy) lambs were anesthetized and catheters were placed into the right and left atrium and main pulmonary artery [as previously described (17)]. An ultrasonic flow probe (Transonics Sytems, Ithaca, NY) was placed around the left pulmonary artery to measure pulmonary blood flow. A vessel loop was placed around the inferior vena cava (IVC) for transient occlusion. Throughout the study, blood gases were obtained at regular intervals; ventilator was adjusted to maintain normal P_{CO_2}. After recovery, the shunt was closed with the use of vascular clips. A 1-h steady-state baseline period was then obtained following instrumentation, before any hemodynamic measurements were made.

At the end of the protocol, all lambs were euthanized with a lethal injection of sodium pentobarbital followed by bilateral thoracotomy as described in the National Institutes of Health Guidelines for the Care and Use of Laboratory Animals. The Committee on Animal Research of the University of California, San Francisco, approved all protocols and procedures.

Hemodynamic measurements. Pulmonary and systemic arterial, and right and left atrial pressures were measured using Sorenson Neonatal Transducers (Abbott Critical Care Systems, N. Chicago, IL). Mean pressures were obtained by electrical integration. Heart rate was measured by a cardiotachometer triggered from the phasic systemic arterial pressure pulse wave. Left pulmonary blood flow was measured with the ultrasonic flowmeter described above. All hemodynamic variables were measured continuously utilizing the Ponemah Physiology Platform (Version 4.9-SP2) with Acquisition Interface, ACQ-7700 (Data Sciences International, St. Paul, MN), and recorded with a Dell Vostro 3500 computer (Dell, Round Rock, TX). Blood gases and pH were measured on a Radiometer ABL5 pH/blood gas analyzer (Radiometer, Copenhagen, Denmark). In shunt lambs, blood gases were obtained from the femoral artery, right ventricle, pulmonary artery, and left atrium. Oxygen saturation and hemoglobin were measured by Co-oximetry (model 682, Instrumentation Laboratory, Lexington, MA), and ratio of pulmonary to systemic blood flow was calculated (Qp:Qs) using the Fick principle. (Mixed venous blood sample was obtained from the RV.) Repeat Qp:Qs measurements were performed to confirm that shunt was occluded in shunt lambs.

Pressure-volume measurements. Admittance pressure-volume catheters (Transonics) were introduced directly into the RV via a ventriculostomy; instantaneous pressure and volume measurements were obtained, which generated pressure-volume (PV) loops (Fig. 1). PV loop interpretation was performed with Labscribe software (iWorx/Labscribe). Each PV loop provided basic measurements of cardiac performance, including heart rate (HR), end-diastolic volume (EDV), end-systolic volume (ESV), stroke volume (SV), and cardiac output. Cardiac output was then normalized to body weight (BW) to obtain cardiac index (CI). Using transient IVC occlusion to adjust preload, a family of PV loops was obtained (Fig. 1*B*). The relationship of the end-systolic points in this family of loops provides the linear end-systolic pressure-volume relationship (ESPVR) with a slope, end-systolic elastance (Ees). ESPVR is load-independent over a wide physiological range, and Ees reflects the ionotropic status of the heart (3). Ventriculoarterial coupling is the matching of ventricular contractility to afterload; it can be quantified using the relationship of Ees to elastance (Ea). For the RV, an Ees/Ea of ~1.5 is considered optimal (14). If contractility is insufficient to meet the demands of increased afterload, the Ees/Ea ratio will decrease. Pressure-volume area (PVA) characterizes the total mechanical work of the ventricle and is defined by the area enclosed by ESPVR, end-diastolic pressure-volume relationship (EDPVR), and the systolic pressure-volume limb of the PV loop (12). It is closely correlated with myocardial oxygen consumption. Ventricular efficiency is the percentage of mechanical work (PVA) converted into external stroke work (SW). SW is defined by the area enclosed by the PV loop. Thus, efficiency is equal to SW/PVA (5).

Pulmonary artery banding (PAB). Following a recovery period, baseline PV measurements were obtained. Using umbilical tape around the main pulmonary artery, the PAB was then constricted to achieve an RV pressure equal to 50% systemic systolic pressure. Throughout the study period, adjustments were made to the PAB to maintain this relationship. PV measurements were then obtained at *time 0* and every 30 min for a total of 240 min. During this period, there were no changes in aortic pressure.

Western blot. Protein extracts from heart tissue were prepared in extraction buffer (20 mM $NaPO_4$, 150 mM NaCl, 2 mM $MgCl_2$, 0.1% Nonidet P-40, 10% glycerol, 10 mM sodium fluoride, 0.1 mM sodium orthovanadate, 10 mM sodium pyrophosphate, 100 μM phenylasine oxide, 10 nm okadaic acid, 1 mM dithiothreitol, 10 μg/ml leupeptin, 10 μg/ml aprotinin, 10 μg/ml pepstatin). Total protein concentrations in the samples were quantified using Nana Drop Spectrophotometer (ND-1000, Thermo Fisher Scientific, Waltham, MA). An equal amount of protein was loaded in each lane for Western blot analysis. Protein samples (10 μg) were subjected to 10% polyacrylamide gel (SDS-PAGE) electrophoresis followed by transfer to a polyvinylidene difluoride (PVDF) membrane. The membranes were then blocked with 5% nonfat dried milk in 130 mM NaCl and 25 mM Tris (TBS, pH 7.5) for 1 h at room temperature. The membranes were incubated in primary antibodies against α-MHC and β-MHC (Santa Cruz Biotechnology, Santa Cruz, CA). Anti-β-actin was used as the protein level of loading controls. The immunoblot was incubated at 4°C overnight and was then washed in TBST. Anti-rabbit IgG or anti-mouse IgG horseradish peroxidase conjugated secondary antibody in TBST-2% goat serum was then added to the incubation for 1 h at 4°C, followed by washing in TBST. Chemiluminescence was then used for visualization of bands (SuperSignal West Pico Chemiluminescent Substrate kit, Thermo Scientific). Quantification of protein band density in X-ray films from ECL Western Blots was performed by a public domain Java image processing program, ImageJ (NIH Image).

Statistical analysis. For heart weight (HW), BW measurements, and Western blot protein analysis, data are shown as means ± SD. For physiological measurements in each animal, measurements for HR, EDV, ESV, SV, and CI are obtained as means from two different time points, each the average of 5–8 cardiac cycles. For Ees, means were obtained for two different measurements at each time point in each animal. Values shown represent the mean of the means ± SE of the mean. Significance was determined with a two-tailed, unpaired *t*-test when comparing between two groups. In Western blot protein analysis between groups and for hemodynamic data comparisons within groups over time, analysis of variance (ANOVA) was used to determine significance when comparing the three groups.

RESULTS

Compared with control lambs, shunt lambs demonstrated biventricular hypertrophy (Fig. 1*A*). Shunt lambs had higher ratios of heart weight (HW) to body weight (BW), RV/BW, and left ventricle (LV)/BW in control vs. shunt lambs, respectively ($P < 0.001$). However, there was no differential hypertrophic response in the RV compared with the LV (Fig. 1*B*). Global cardiac hypertrophy in shunt lambs was apparent when comparing intact hearts (Fig. 1*C*), and biventricular hypertro-

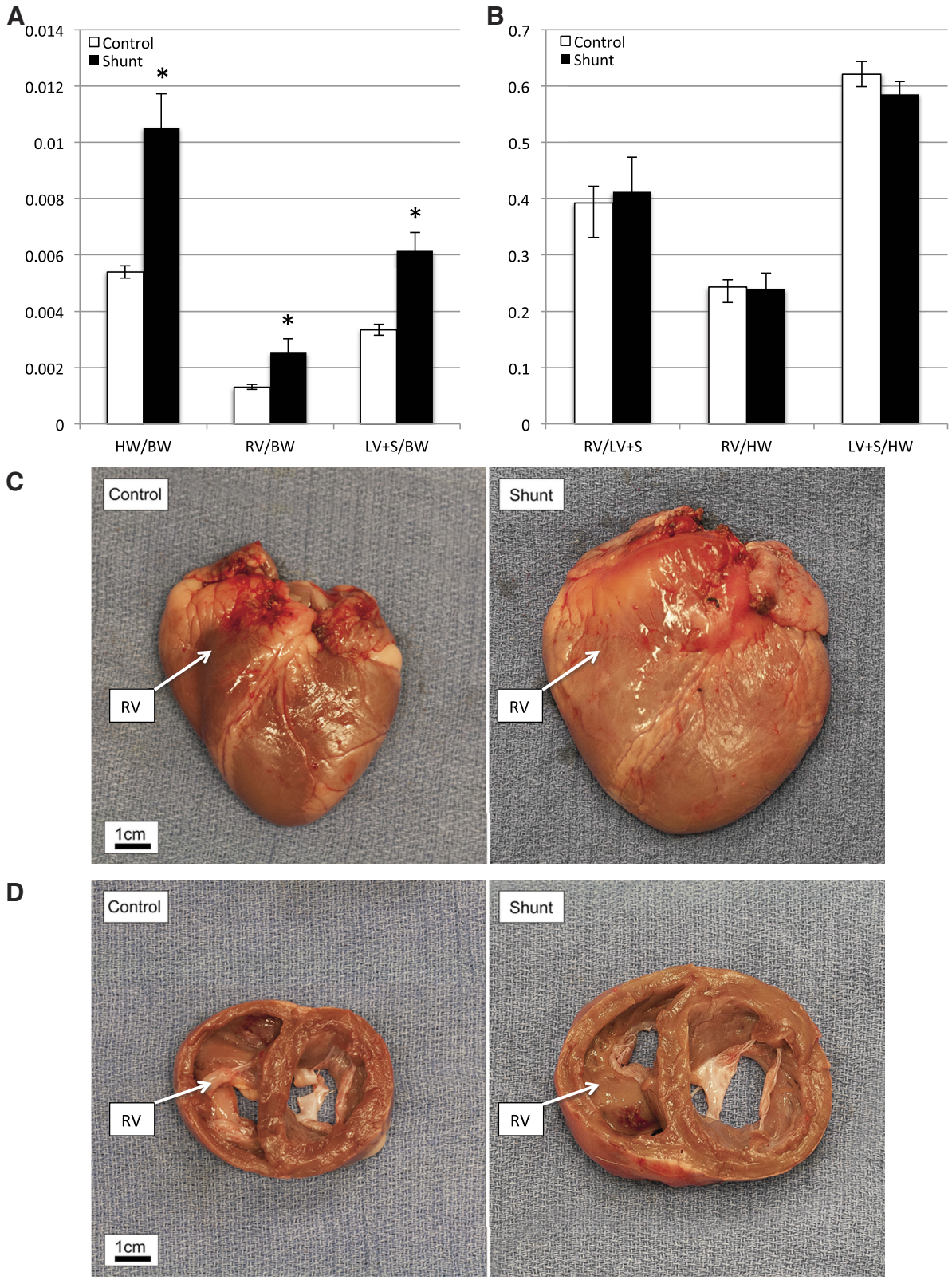

Fig. 1. *A*: compared with control lambs, shunt lambs have increased total heart weight (HW)-to-body weight (BW) ratio. Both right ventricle (RV) and left ventricle plus septum (LV + S) weights are increased relative to BW. Values are means ± SD; $n = 6$ in each group. *$P < 0.05$. *B*: there are no differences between shunt and control lambs in the ratio of RV to LV + S weight, or RV and LV + S weight to total heart weight, suggesting no differential hypertrophic response in the RV compared with the LV. Values are means ± SD; $n = 6$ in each group. For *C* and *D*, control lamb BW = 10.2 kg, HW = 56.5 g; shunt lamb BW = 10.9 kg, HW = 121.4 g. RV in each panel is labeled. *C*: gross picture of control lamb heart (*left*) and shunt lamb heart. *D*: gross picture of 2-cm section through left and right ventricles starting at atrioventricular (AV) grove, control (*left*), and shunt.

Table 1. *Baseline hemodynamics in control and shunt lambs*

	Control	Shunt Open	Shunt Closed	*P* Value (Shunt Open vs. Control)	*P* Value (Shunt Closed vs. Control)
SBP, mmHg	66.3 ± 2.1	55.7 ± 3.5	72.8 ± 7.7	0.02*	0.40
DBP, mmHg	54.6 ± 2.4	29.0 ± 2.1	58.3 ± 8.4	<0.001*	0.65
LPBF, L/min	0.50 ± 0.06	2.12 ± 0.21	0.96 ± 0.16	<0.001*	0.02*
PAP, mmHg	11.8 ± 0.8	23.7 ± 2.4	15.7 ± 2.6	<0.001*	0.16
LAP, mmHg	4.9 ± 0.64	11.2 ± 1.7	4.7 ± 1.0	<0.01*	0.81
RAP, mmHg	2.9 ± 0.6	3.2 ± 0.6	2.2 ± 0.4	0.82	0.37
HR, beats/min	133.7 ± 4.3	136.7 ± 6.2	130.8 ± 7.3	0.70	0.73

Values are expressed as means ± SE of mean; $n = 6$ in each group. SBP, systolic blood pressure; DBP, diastolic blood pressure; LPBF, left pulmonary blood flow; PAP, pulmonary artery pressure; LAP, left atrial pressure; RAP, right atrial pressure; HR, heart rate. *Significant difference.

phy was demonstrated on gross pathological section (Fig. 1*D*). Anatomic examination of the heart and great vessels of lambs revealed no atrial septal defects, patent foramina ovalia, or patent ductus arteriosi.

Shunt lambs had a pulmonary to systemic blood flow (Qp: Qs) ratio of 2.9 ± 1.3 before closure, which was decreased to 1.1 ± 0.2 after shunt occlusion. Consistent with prior studies, at baseline, shunt lambs had significantly increased left pulmonary blood flow, pulmonary artery pressure, and left atrial pressure, compared with control lambs. Mean systolic pressure was lower in shunt lambs due to lower diastolic blood pressure; these differences were abolished with shunt closure. In fact, other than LPBF, there were no baseline differences in control and shunt lambs after shunt closure (Table 1). Hemoglobin was measured at the beginning of the study and was significantly higher in control compared with shunt lambs (9.1 ± 1.0 vs. 7.6 ± 1.3 g/dl, $P = 0.02$.) There were no differences between pH, Po_2, Pco_2, or bicarbonate between the groups (data not shown).

After shunt closure, baseline PV loops were obtained in control and shunt lambs (Fig. 2*A* and Table 2). Shunt lambs had greater EDV, ESV, and SV ($P < 0.05$). The disparate volumes at baseline were likely reflective of the global cardiac hypertrophy seen in shunt lambs. CI was greater in shunt lambs compared with controls, while there were no baseline differences in HR. Ees was lower, but PVA was greater in shunt than control lambs, while there were no differences in ventricular efficiency. There were no differences in EDPVR (data not shown).

Following baseline measurements, PAB was constricted until maximum RV pressure was equal to 50% baseline systemic systolic pressure (Fig. 3). This level of constriction was maintained for 240 min, with PV loop measurements obtained every 30 min. Although shunt lambs continued to have increased absolute cardiac index at 240 min (Table 3, Fig. 4*A*, 116.2 ± 18.1 vs. 258.2 ± 55.3 ml·min^{-1}·kg BW^{-1}, $P = 0.05$), both control and shunt lambs had similar increases in cardiac index compared with baseline (1.57 vs. 1.54, control vs. shunt, respectively, $P = 0.48$). However, control lambs demonstrated increased HR with PAB (Table 3, Fig. 4*B*, 168.9 ± 7.3 vs. 138.7 ± 6.6 beats/min, $P = 0.01$). In contrast, shunt lambs had increased inotropy compared with baseline, as reflected by Ees (Fig. 4*C*, 1.31 ± 0.2 × baseline control vs. 2.63 ± 0.46 ×

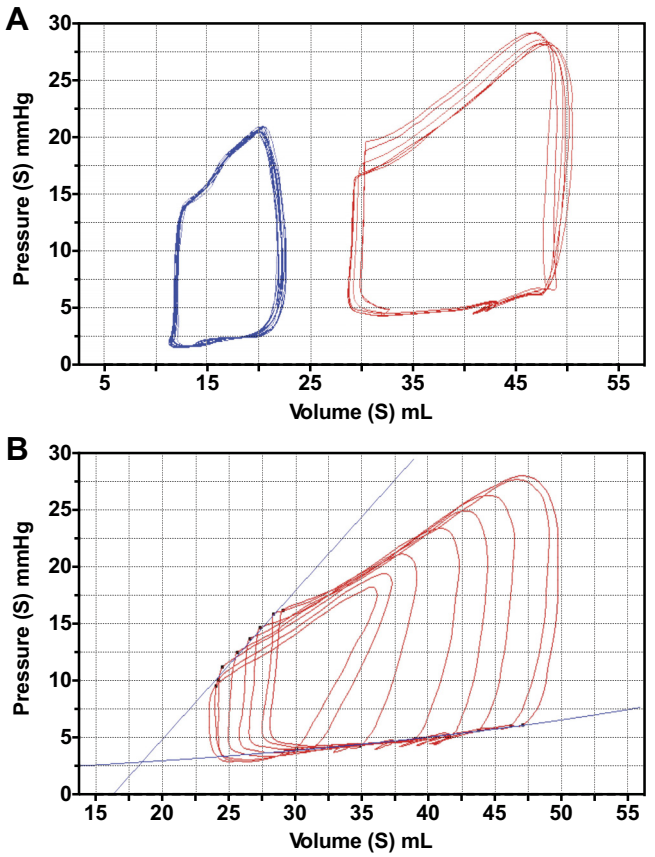

Fig. 2. *A*: baseline pressure-volume (PV) loops in control lambs (blue) and shunt lambs (red). Loops are obtained at steady state with a pause in ventilation to reduce artifact. Analyses are done using the average of 5–8 cardiac cycles, as shown. *B*: shunt loops demonstrating transient inferior vena caval (IVC) occlusion. A family of PV loops is generated by alterations in preload. End-systolic pressure-volume relationship (ESPVR) and end-diastolic pressure-volume relationship (EDPVR) lines are shown.

Table 2. *Baseline hemodynamics derived from PV analysis in control and shunt lambs*

	Control	Shunt	*P* Value
EDV, ml	22.8 ± 5.9	48.7 ± 10.0	0.01*
ESV, ml	14.4 ± 1.4	33.5 ± 9.8	0.04*
SV, ml	8.7 ± 1.8	15.8 ± 2.7	0.04*
CI, ml·min^{-1}·kg BW^{-1}	73.9 ± 4.0	159.2 ± 25.1	0.04*
HR, beats/min	131.8 ± 3.7	129.0 ± 10.7	0.81
Ees	2.3 ± 0.44	1.16 ± 0.32	0.02*
PVA, mJ	0.026 ± 0.0079	0.063 ± 0.013	0.03*
Efficiency, %	89.6 ± 5.6	80.2 ± 7.7	0.18

Values are expressed as mean of means ± SE of mean; $n = 6$ in each group. EDV, end-diastolic volume; ESV, end-systolic volume; SV, stroke volume; CI, cardiac index; BW, body weight; Ees, end elastance (slope of end-systolic pressure-volume relationship); HR, heart rate; PVA, pressure volume area. Efficiency = stroke work/PVA. *Significant difference.

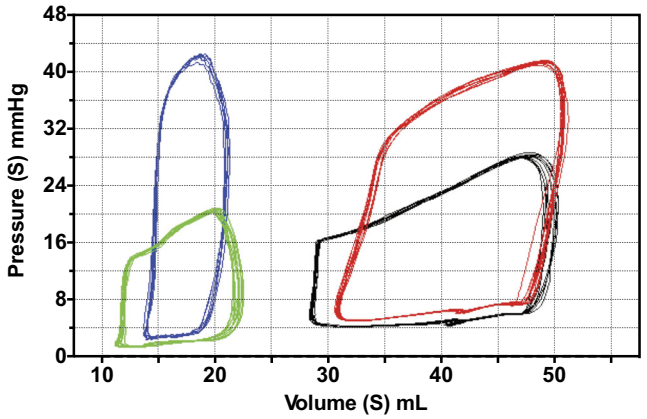

Fig. 3. Representative PV loops after pulmonary artery band (PAB) tightening. Control lamb at baseline (green) and at *time 0* (blue). Shunt lamb at baseline (black) and at *time 0* (red).

baseline, $P = 0.02$). Control and shunt lambs demonstrate similar changes (relative to baseline) in Ea (3.16 ± 1.05-fold vs. 2.98 ± 1.52-fold baseline, $P = 0.82$). Given the concomitant increase in Ees in shunt, but not control, lambs, the Ees/Ea ratio is preserved (0.99 ± 0.28-fold baseline, $P = 0.04$, compared with controls). In contrast, control lambs demonstrate a marked decrease in the Ees/Ea ratio (0.63 ± 0.06-fold baseline), reflective of RV-arterial uncoupling. Furthermore, shunt lambs demonstrated greater PVA at baseline compared with controls (Table 2). Both shunt and control lambs increased PVA relative to baseline after acute afterload challenge with PAB, but the extent of increase was much greater in controls than shunts (Fig. 5*B*, 5.3 ± 1.8-fold baseline vs. 2.03 ± 0.3-fold baseline, $P = 0.05$). Consequently, although there were no differences in efficiency at baseline between shunt and control lambs (Fig. 5*A*, Table 2), shunt lambs maintained efficiency compared with baseline, while controls exhibited a drop in efficiency after PAB (Fig. 5*C*, 0.71 ± 0.06-fold baseline vs. 0.99 ± 0.08-fold baseline, $P = 0.02$).

We hypothesize that the mechanical effects demonstrated by this study are reflective of a retained physiological and biochemical fetal phenotype in the RV of shunt lambs. To begin to investigate these changes, we assessed α-myosin heavy chain (MHC) and β-MHC expression. Classically, α-MHC is associated with the adult myocardial phenotype, in both the LV and RV, while β-MHC is associated with the fetal phenotype. In shunt lambs, LV α-MHC expression is similar to that of controls. However, RV α-MHC expression is decreased in shunts, with no difference between shunt and fetal RV expression levels (Fig. 6*A*). Furthermore, in both the RV and LV of shunt lambs, β-MHC expression is decreased, compared with controls; there are no differences between fetal and shunt RV β-MHC expression, while β-MHC is decreased in fetal LV compared with shunt LV (Fig. 6*B*). This MHC expression pattern reflects a retained fetal phenotype in the shunt RV.

DISCUSSION

While it has long been known that survival in patients with PAH associated with CHD is superior compared with other forms of PAH, despite similar pulmonary vascular hemodynamics (8), the mechanisms that might account for this difference are unknown and have been the subject of limited investigation. One potential mechanism might be "maladaptive" in that the presence of a communication at either the atrial or ventricular level (or both) allows right-to-left shunting of blood, preserving left-sided output during right ventricular failure. However, others have suggested that increased RV pressure or volume loading from birth leads to an adaptive response within the RV myocardium, which leads to improved ability to respond to chronically altered afterload when PAH develops (9, 10). Investigating these potential mechanisms is important, given the need to develop rational and effective therapeutic strategies for PAH patients with and without CHD. For example, if the atrial or ventricular communication is paramount, then earlier atrial septostomy may be advocated (15). However, if an adaptive ventricular response is vital, then exploration of its mechanisms may provide novel RV therapeutic targets in the setting of PAH associated with CHD. We studied the latter by utilizing a unique lamb model of CHD with increased pulmonary blood flow (shunt), to examine differences compared with controls in RV responses to increased afterload over a 4-h period. Using this model, we were able to demonstrate markedly different patterns of response, the control RV maintaining cardiac output via maladaptive mechanisms of increased heart rate and reduced mechanical efficiency while in the previously shunted RV the increase in cardiac output was adaptive, associated with a gradual increase in contractility, presumably via an enhanced Anrep effect.

Response to afterload in the normal left ventricle is biphasic and time dependent. After an acute physiological increase in aortic pressure, there is a rapid increase in developed force related to increased myocardial calcium sensitivity (Frank-starling mechanism), followed by a second, more gradual, increase in force development (Anrep effect). The left ventricular Anrep effect is largely responsible for the maintained stroke volume seen during changes in systemic arterial pressure, and its underlying autocrine and paracrine mechanisms have been investigated extensively and recently have been

Table 3. *Hemodynamics after PAB (relative to pre-PAB) in control and shunt lambs*

	Control		Shunt	
	Immediately after PAB	240 min after PAB	Immediately after PAB	240 min after PAB
CI, ml·min^{-1}·kg BW^{-1}	0.97 ± 0.08	1.57 ± 0.23*	0.81 ± 0.21	1.54 ± 0.12*
SV, ml	0.85 ± 0.09	1.27 ± 0.22	0.77 ± 0.12	1.25 ± 0.19
HR, beats/min	1.07 ± 0.02*	1.22 ± 0.05*	1.01 ± 0.06	1.11 ± 0.05
ESV, ml	1.34 ± 0.08*	1.41 ± 0.31	1.17 ± 0.08	1.18 ± 0.12
EDV, ml	1.24 ± 0.07	1.32 ± 0.33	1.32 ± 0.18	1.23 ± 0.11

Values are expressed as mean of means ± SE of mean; $n = 6$ in each group. Values for CI, SV, HR, ESV, and EDV are shown relative to baseline. PAB, pulmonary artery band. *$P < 0.05$ compared with baseline determined by ANOVA.

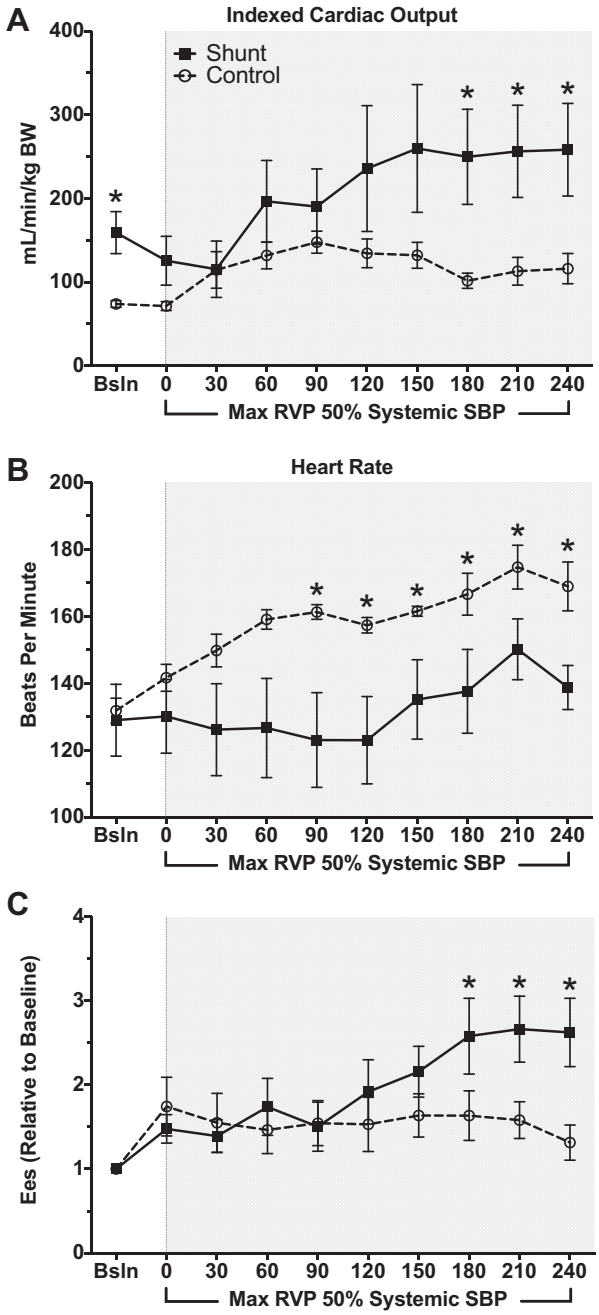

Fig. 4. All data shown begin with baseline, then every 30 min after PAB tightening to RVP systolic pressure 50% systemic systolic pressure. *A*: cardiac output, indexed to body weight, in shunts vs. controls. Both at baseline and at 180, 210, and 240 min, shunt lambs have increased cardiac output compared with control lambs. *B*: beginning 90 min after PAB tightening, and continuing until 240 min, HR in control lambs is higher than that of shunt lambs. *C*: Ees, the slope of ESPVR, is higher in shunt lambs compared with control lambs beginning at 180 min after PAB and continuing until 240 min. $*P < 0.05$, shunt vs. control. Values are means ± SE of mean; $n = 6$ in each group.

reviewed in detail (4). Very little is known about the Anrep effect in the normal RV. However, in a study using single beat analysis of RV contractility in dogs, modest changes in RV afterload resulting from hypoxia and clamping of the pulmonary artery to less than half systemic pressure led to a small increase in Ees, suggestive of an Anrep effect (2). Our PA banding protocol was associated with a larger increase in PA pressure and was not associated with a significant increase in Ees in the RV of controls. This suggests that, at least in the normal heart, there may be a threshold of afterload beyond which an adaptive Anrep mechanism cannot compensate, and in our studies maladaptive responses predominated. This would be compatible with the well-known increased afterload sensitivity of the normal RV compared with the LV (11).

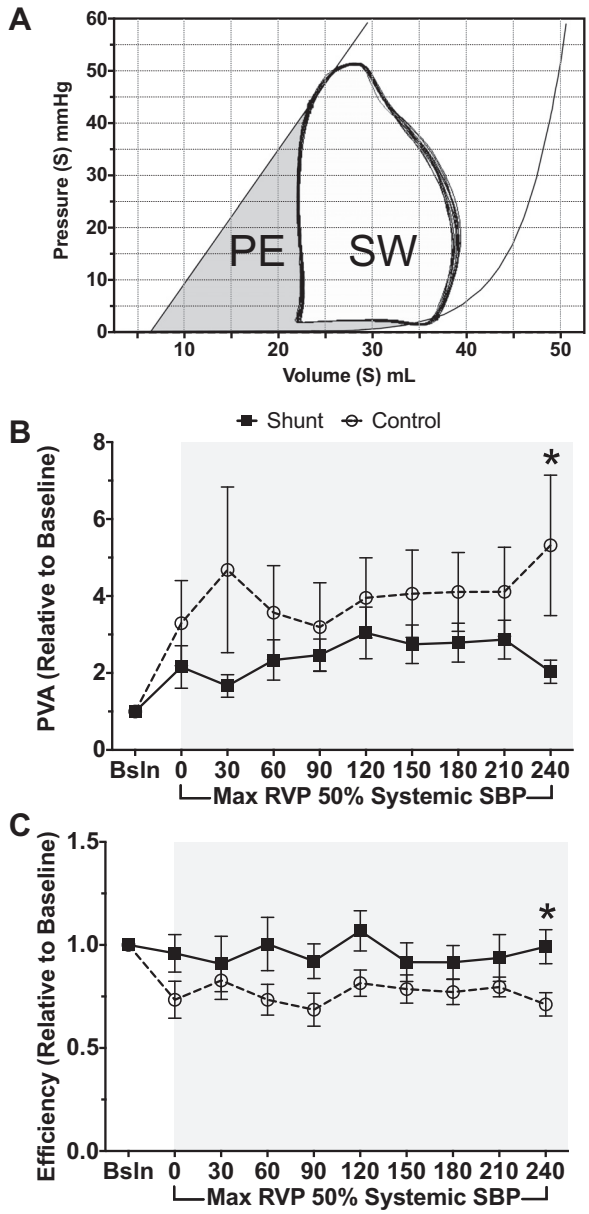

Fig. 5. *A*: pressure-volume area (PVA) and ventricular efficiency demonstrated with a representative loop. PVA is represented by the total shaded area, bound by the ESPVR, end-diastolic pressure volume relations, and the systolic limb of the PV loop. PVA reflects total mechanical work of the ventricle, which includes external stroke work (SW) in the area bound by the PV loop and potential energy (PE). Ventricular efficiency is the ratio of SW to total mechanical work, or SW/PVA. *B*: PVA. After 240 min of PAB, PVA increases by 5.3-fold baseline in control animals, while shunt animals have a lesser increase of 2.3-fold baseline with PAB. *C*: ventricular efficiency. After 240 min of PAB, shunt animals maintain efficiency (0.99-fold baseline) while control animals suffer decreased efficiency (0.71-fold baseline). $*P \leq 0.05$, shunt vs. control. Values are means ± SE of mean; $n = 6$ in each group.

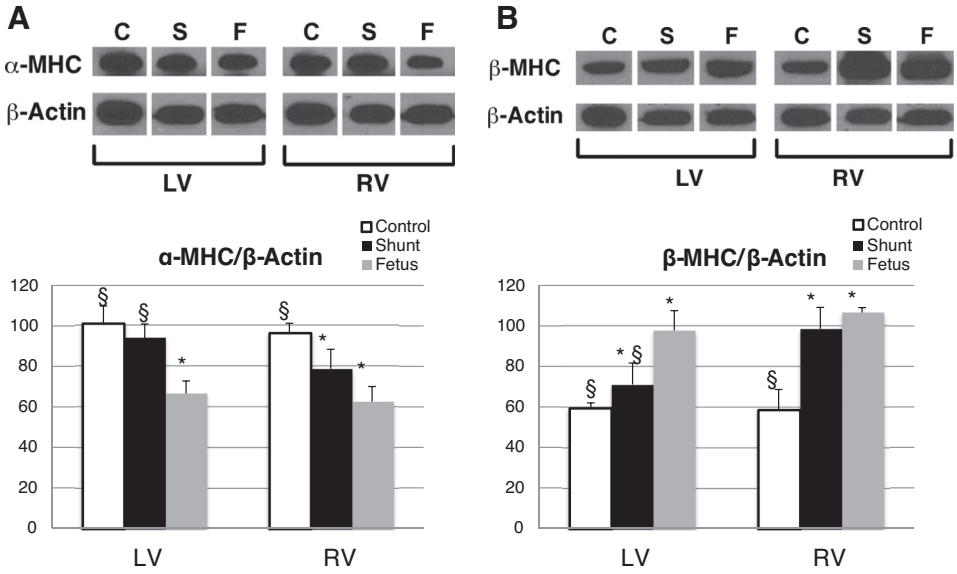

Fig. 6. Myosin heavy chain (MHC) expression. *A*: shunt RV expression of α-MHC is decreased compared with control RV to levels similar to the fetal RV. There are no changes in shunt LV α-MHC expression. *B*: shunt LV and RV expression of β-MHC is increased compared with controls; although shunt LV β-MHC is decreased compared with fetal LV, there is no difference between fetal and shunt RV β-MHC expression. *$P < 0.05$ compared with control, §$P < 0.05$ compared with fetus. The bar graphs represent densitometry performed on individual samples; values are means ± SD, $n = 5$ in each group. Blots are rearranged to be grouped by chamber. C, control; S, shunt; F, fetal.

Conversely, in our shunt group, PA banding was associated with a robust, continued, two-and-a-half-fold increase in Ees over the course of the 4-h study period. Given that both control and shunt lambs experienced similar increases in Ea with PAB, the increase in Ees in shunt lambs resulted in preserved ventriculoarterial coupling, while the Ees/Ea relationship decreased in control lambs after PAB, reflecting ventriculoarterial uncoupling. This strongly suggests that the chronic hemodynamic responses associated with in utero shunting and postnatal adaptation in our model of CHD lead to markedly different myocardial properties manifest, in part, by enhancement of the Anrep effect and improved adaptive responses to changes in afterload.

While not designed to examine cellular mechanisms, these findings are consistent with the known hemodynamic consequences of CHD with shunt lesions. In the fetus, the RV is the dominant ventricle, supplying approximately two-thirds of combined cardiac output, with mean pulmonary arterial pressure ~2 mmHg greater than systemic pressure (20). During the normal transition from intrauterine to postnatal circulation, RV afterload is drastically reduced as pulmonary vascular resistance falls, and the RV is altered, both morphologically and mechanically, to efficiently deliver cardiac output to this low-resistance circuit, with minimal work, energy requirements, and oxygen consumption compared with the normal LV. Within 24 h after birth, mean pulmonary arterial pressure falls to ~50% of systemic values, reaching an adult nadir within 2–3 wk (18, 21). In contrast, in the setting of a posttricuspid level left-to-right shunt, as in our model of CHD created by the in utero placement of an aorta-to-pulmonary shunt, the RV is continually exposed to systemic-level afterload, and thus may be both anatomically and physiologically more adapted to increased afterload. Importantly, shunt placement in our model does not alter fetal hemodynamics; ~50% of normal flow through the ductus arteriosus passes through the aortopulmonary shunt (unpublished observations). However, the shunt is in place during spontaneous delivery, which exposes the RV to the flow and pressure stimulus immediately after birth, recapitulating the scenario of CHD. In the present study (consistent with prior studies) shunt lambs had biventricular hypertrophy compared with control lambs (1). Commensurate with observed myocardial size, we found that volumetric indexes were consistently higher in shunt lambs, including EDV, ESV, and SV. As there were no baseline differences in HR, it follows that CI was also greater in shunt lambs compared with controls. Despite this increased CI, Ees was lower at baseline in shunt than control lambs. While this may reflect a lower baseline inotropic state and improved inotropic reserve in shunt lambs, it may simply be a manifestation of the known inverse relationship between Ees and ventricular size (23). More importantly, the pattern of change in Ees following banding, discussed above, was markedly different despite little change in ventricular volume without differences in total RV preload.

Nonetheless, shunt lambs had higher per-beat RV oxygen consumption at baseline, as defined by PVA. This was not surprising, given the greater stroke work, higher cardiac output, and greater RV mass (relative to BW) in shunt lambs relative to controls. However, when challenged with the stimulus of increased afterload, controls had a greater increase in PVA compared with shunts, suggesting greater physiological strain under these circumstances. As PVA only estimates the mechanical work done in one cardiac cycle and does not account for HR, the total mechanical work (and thus total myocardial oxygen consumption) of the control lambs was even greater, given the tachycardic response in these animals with PAB. Further, while the RV of shunt lambs continued to be highly efficient despite increased afterload, control lambs suffered a drop in efficiency to 71% of baseline levels, suggesting further, probably interrelated maladaptive responses to increased afterload.

There are several noteworthy limitations to the current study. First, the acute afterload stimulus applied with PAB is more akin to that seen in pulmonary embolus or surgical interventions for CHD. Although these are physiologically relevant situations in certain patient populations, the stimulus is not equivalent to that of a more gradual elevation in PVR in PAH. Future studies are needed to recapitulate a more gradual, chronic increase in RV afterload. Also, the afterload applied by

PAB is "passive," as opposed to distal "active" afterload seen with arteriopathy in PAH, and this may have particular relevance in terms of differences in imposed hydraulic impedance and ventriculovascular coupling of the RV (7). Our data must be interpreted with caution therefore, although it is unlikely that our central finding of a marked difference in Ees response and enhanced Anrep effect would be influenced significantly by the mode of afterload increase. In this regard, and briefly discussed earlier, our experiments were not designed to examine the autocrine, paracrine, and cell-signaling responses associated with changes in Anrep effects previously shown for the LV. Our data provide novel data on which future such studies could be based. Finally, we did not examine effects of increased RV afterload on LV performance or examine ventricular interdependence. This is an important limitation, as the two ventricles are inexorably related, sharing muscle fibers, the interventricular septum, and enclosed within the same pericardium (22). Future studies to characterize the complex physiological interplay between the ventricles under conditions of RV strain and failure are warranted. While expression patterns of α-MHC and β-MHC in the shunt RV reflects a retained fetal phenotype, examination of these genes alone is incomplete and does not explain the adaptive mechanical response of the shunt RV demonstrated in this study. Future investigations remain to be done to examine canonical pathways involved in PAH and heart failure in the RV of fetal and shunt lambs and to undertake genome analysis. Such studies may yield novel molecular therapeutic targets for the failing RV.

In summary, using a unique lamb model of CHD with chronic left-to-right shunt, we have characterized a novel adaptive and sustainable RV physiological response to acute PAB, manifest by an enhanced Anrep effect. As all current therapies for PH are focused on reversing or attenuating the progression of pulmonary vascular arteriopathy, rather than specifically supporting RV function, a more thorough understanding of the pathobiological mechanisms underlying the RV response characterized in this model may have important therapeutic implications.

ACKNOWLEDGMENTS

We thank L. Talkin and the UC Davis Veterinary Staff for excellent animal care. We are grateful to J. Hoffman, MD, for critical reading of the article and statistical advice.

GRANTS

This research was supported in part by grants from the National Institutes of Health (HL-61284 to J. R. Fineman and 5T32-HD-049303-07 to J. R. Fineman and R. C. Johnson).

DISCLOSURES

No conflicts of interest, financial or otherwise, are declared by the author(s).

AUTHOR CONTRIBUTIONS

Author contributions: R.C.J., P.E.O., S.H.B., A.N.R., and J.R.F. conception and design of research; R.C.J., S.A.D., J.M., C.E.S., M.J.J., Y.H., and G.W.R. performed experiments; R.C.J., S.H.B., C.E.S., Y.H., and J.R.F. analyzed data; R.C.J., S.A.D., P.E.O., S.H.B., Y.H., A.N.R., and J.R.F. interpreted results of experiments; R.C.J., S.H.B., C.E.S., and Y.H. prepared figures; R.C.J. drafted manuscript; R.C.J., S.A.D., P.E.O., Y.H., A.N.R., and J.R.F. edited and revised manuscript; R.C.J., S.A.D., P.E.O., S.H.B., J.M., C.E.S., M.J.J., Y.H., G.W.R., A.N.R., and J.R.F. approved final version of manuscript.

REFERENCES

1. **Azakie A, Fineman JR, He Y.** Myocardial transcription factors are modulated during pathologic cardiac hypertrophy in vivo. *J Thorac Cardiovasc Surg* 132: 1262–1271, e4, 2006.
2. **Brimioulle S, Wauthy P, Ewalenko P, Rondelet B, Vermeulen F, Kerbaul F, Naeije R.** Single-beat estimation of right ventricular end-systolic pressure-volume relationship. *Am J Physiol Heart Circ Physiol* 284: H1625–H1630, 2003.
3. **Burkhoff D.** Assessment of systolic and diastolic ventricular properties via pressure-volume analysis: a guide for clinical, translational, and basic researchers. *Am J Physiol Heart Circ Physiol* 289: H501–H512, 2005.
4. **Cingolani HE, Perez NG, Cingolani OH, Ennis IL.** The Anrep effect: 100 years later. *Am J Physiol Heart Circ Physiol* 304: H175–H182, 2013.
5. **Gaemperli O, Biaggi P, Gugelmann R, Osranek M, Schreuder JJ, Bühler I, Sürder D, Lüscher TF, Felix C, Bettex D, Grünenfelder J, Corti R.** Real-time left ventricular pressure-volume loops during percutaneous mitral valve repair with the MitraClip system. *Circulation* 127: 1018–1027, 2013.
6. **Ghio S, Gavazzi A, Campana C, Inserra C, Klersy C, Sebastiani R, Arbustini E, Recusani F, Tavazzi L.** Independent and additive prognostic value of right ventricular systolic function and pulmonary artery pressure in patients with chronic heart failure. *J Am Coll Cardiol* 37: 183–188, 2001.
7. **Grignola JC.** Assessment of right ventricular afterload by pressure waveform analysis in acute pulmonary hypertension. *World J Cardiol* 3: 322, 2011.
8. **Hopkins WE, Ochoa LL, Richardson GW, Trulock EP.** Comparison of the hemodynamics and survival of adults with severe primary pulmonary hypertension or Eisenmenger syndrome. *J Heart Lung Transplant* 15: 100–105, 1996.
9. **Hopkins WE.** The remarkable right ventricle of patients with Eisenmenger syndrome. *Coron Artery Dis* 16: 19–25, 2005.
10. **Hopkins WE.** Right ventricular performance in congenital heart disease: a physiologic and pathophysiologic perspective. *Cardiol Clinics* 30: 205–218, 2012.
11. **MacNee W.** Pathophysiology of cor pulmonale in chronic obstructive pulmonary disease. Part I. *Am J Respir Crit Care Med* 150: 833–852, 1994.
12. **Nozawa T, Yasumura Y, Futaki S, Tanaka N, Uenishi M, Suga H.** Efficiency of energy transfer from pressure-volume area to external mechanical work increases with contractile state and decreases with afterload in the left ventricle of the anesthetized closed-chest dog. *Circulation* 77: 1116–1124, 1988.
13. **Oishi P, Datar SA, Fineman JR.** Advances in the management of pediatric pulmonary hypertension. *Respir Care* 56: 1314–1339, discussion 1339–1340, 2011.
14. **Pagnamenta A, Dewachter C, McEntee K, Fesler P, Brimioulle S, Naeije R.** Early right ventriculo-arterial uncoupling in borderline pulmonary hypertension on experimental heart failure. *J Appl Physiol* 109: 1080–1085, 2010.
15. **Bhamra-Ariza P, Keogh AM, Muller DW.** Percutaneous interventional therapies for the treatment of patients with severe pulmonary hypertension. *J Am Coll Cardiol* 63: 611–618, 2014.
16. **Rabinovitch M.** Molecular pathogenesis of pulmonary arterial hypertension. *J Clin Invest* 122: 4306–4313, 2012.
17. **Reddy VM, Meyrick B, Wong J, Khoor A, Liddicoat JR, Hanley FL, Fineman JR.** In utero placement of aortopulmonary shunts. A model of postnatal pulmonary hypertension with increased pulmonary blood flow in lambs. *Circulation* 92: 606–613, 1995.
18. **Redington AN.** Right ventricular function. *Cardiol Clinics* 20: 341–349, v, 2002.
19. **Roche SL, Redington AN.** The failing right ventricle in congenital heart disease. *Can J Cardiol* 29: 768–778, 2013.
20. **Rudolph AM, Heymann MA.** Circulatory changes during growth in the fetal lamb. *Circ Res* 26: 289–299, 1970.
21. **Rudolph AM.** The changes in the circulation after birth: their importance in congenital heart disease. *Circulation* 41: 343–359, 1970.
22. **Sheehan F, Redington A.** The right ventricle: anatomy, physiology and clinical imaging. *Heart* 94: 1510–1515, 2008.
23. **Starling MR, Mancini GB, Montgomery DG, Gross MD.** Radionuclide left ventricular contractile indices and their relationship to heart size in dogs. *Am Heart J* 118: 325–333, 1989.

24. **Thenappan T, Shah SJ, Rich S, Gomberg-Maitland M.** A USA-based registry for pulmonary arterial hypertension: 1982–2006. *Eur Respir J* 30: 1103–1110, 2007.
25. **Voelkel NF, Quaife RA, Leinwand LA, Barst RJ, McGoon MD, Meldrum DR, Dupuis J, Long CS, Rubin LJ, Smart FW, Suzuki YJ, Gladwin M, Denholm EM, Gail DB.** Right ventricular function and failure: report of a National Heart, Lung, and Blood Institute Working Group on Cellular and Molecular Mechanisms of Right Heart Failure. *Circulation* 114: 1883–1891, 2006.
26. **Vonk Noordegraaf A, Galiè N.** The role of the right ventricle in pulmonary arterial hypertension. *Eur Respir Rev* 20: 243–253, 2011.